ELSEVIER

Journal of Chromatography A, 716 (1995) 401–412

JOURNAL OF CHROMATOGRAPHY A

Capillary zone electrophoretic resolution of recombinant human bone morphogenetic protein 2 glycoforms An investigation into the separation mechanisms for an exquisite separation

Kalvin Yim*, Joan Abrams, Amy Hsu

Genetics Institute, 1 Burtt Road, Andover, MA 01810, USA

Abstract

Recombinant human bone morphogenetic protein 2 (rhBMP-2) is a disulfide-linked homodimeric glycoprotein (M_r = 30 000) which induces bone formation in vivo in several animal model systems. In this paper, we report the separation of a homogeneous rhBMP-2 sample into nine peaks by capillary zone electrophoresis (CZE), using a simple, pH 2.5, phosphate buffer containing no additives. The nine peaks have been identified to be glycoforms of rhBMP-2 [designated as $(rhBMP\text{-}2)_2\text{-}(GlcNAc)_4(Man_Z)$, where Z varies from 10 to 18]. The difference between any adjacent pair of peaks is only one mannose residue (M_r = 162). The ability of CZE to resolve rhBMP-2 glycoforms having the same charge and differing only 0.5% in molecular mass, without resorting to chemical complexation, is both unexpected and intriguing. Possible mechanisms explaining how the additional mannose can affect the mobility of rhBMP-2 glycoforms were explored. Zeta potentials of various glycoforms were calculated from their mobilities and interpreted in light of diffuse double layer parameters. Our results suggest that CZE employing a low-pH buffer, where proteins are highly charged, may be uniquely suitable for complex protein glycoform analysis.

1. Introduction

1.1. Overview

Glycoproteins usually exist as heterogeneous populations of glycosylated variants (glycoforms) in which assemblies of different oligosaccharides are attached to each glycosylation site post-translationally. There is increasing evidence that the carbohydrate moieties of glycoproteins play major roles in their structures and functions [1–3]. Traditionally, glycans are studied only after they are enzymatically released from the glycoproteins. High-performance capillary zone electrophoresis (CZE) is emerging as a technique for studying intact glycoproteins [4–12]. Glycoform analysis is particularly challenging because of the enormous diversity of oligosaccharide structures. For example, four different amino acids can only form 24 different tetrapeptides, whereas four different monosaccharides can form 36 000 tetrasaccharides.

There have been numerous reports on the separation of protein glycoforms using CZE [4–9]. However, the identities of the resolved peaks were generally not reported. As a result, it is

* Corresponding author.

0021-9673/95/$09.50
SSDI 0021-9673(95)00742-3

difficult to appraise how difficult a given situation was and how successful the separation was. One notable exception is the reports by Rudd et al. [10–12], who reported the separation of five ribonuclease B glycoforms (designated as RNase Man-5, -6, -7, -8, and -9) by CZE using a buffer containing 20 m*M* sodium phosphate, 50 m*M* SDS, and 5 m*M* sodium tetraborate at pH 7.2. In this study, the glycoforms were separated on the basis of charge differences. Negatively charged borate–oligomannose complexes introduced charge differences among the glycoforms which enabled their separation.

Due to the high purity of our samples, we can identify all the peaks in the electropherogram and rule out the possibility of sample contamination or degradation. As a result, we can demonstrate that we can separate all the rhBMP-2 glycoforms according to their number of mannose residues and that glycoforms that have the same number of mannose residues cannot be resolved by our CZE system. We also estimated that the effect of an additional mannose on rhBMP-2 mobility is equivalent to about half a charge.

1.2. rhBMP-2 structure

Recombinant human bone morphogenetic protein 2 (rhBMP-2) is an $M_r = 30\,000$, *homodimeric* basic protein ($pI > 8.5$) which has been shown to induce bone growth in vivo in several animal models [13–19]. Implantation of rhBMP-2 in the rat ectopic model induced bone formation within 14 days [19]. This protein presumably transforms primitive mesenchymal cells into osteoblasts that form host bone. Fig. 1 is a schematic diagram of the primary structure of rhBMP-2. Each *monomer* subunit contains 114 amino acids including 7 cysteines and 1 Asn-X-Ser/The consensus glycosylation site at Asn^{56}. The highlighted sequence constitutes the D5 glycopeptide spanning from D^{53} to L^{92}. The N-terminus of rhBMP-2 is a glutamine (Gln) which can cyclize to form a pyroglutamic acid (pyroglu). rhBMP-2 normally exists as a homodimer via the C^{78}–C^{78} interchain disulfide bond. Fig. 2 is a schematic diagram of an N-linked

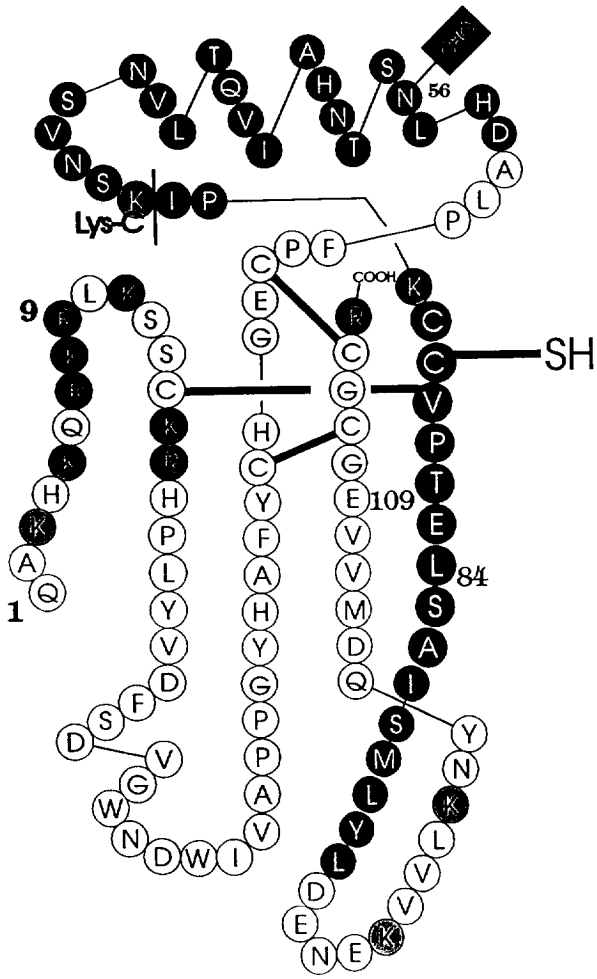

Fig. 1. Primary structure of recombinant human bone morphogenetic protein 2 (rhBMP-2).

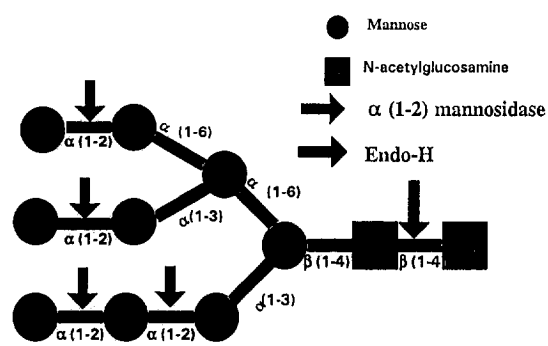

Fig. 2. A diagrammatic representation of an oligomannose 9 structure showing endoglycosidase H (Endo-H) and α(1–2)mannosidase cleavage sites.

oligomannose 9 structure with the endoglycosidase H (Endo-H) and α(1–2)mannosidase cleavage sites indicated, respectively.

1.3. Diffuse double layer model

Fig. 3 models a diffuse double layer around a charged colloidal particle, a protein molecule, for instance, in an electrolyte solution. In any electrolyte solution, there are counterions. Some counterions may be associated rather tightly (fixed diffuse layer), while others more loosely (mobile diffuse layer). The electrolyte forms an ion atmosphere around the particle, the ion atmosphere can effectively reduce the net charge on the protein because oppositely charged ions will tend to be attracted to the protein. The interface between the fixed portion of diffuse layer and the mobile portion of diffuse layer is called the surface of shear or the slip plane. It is

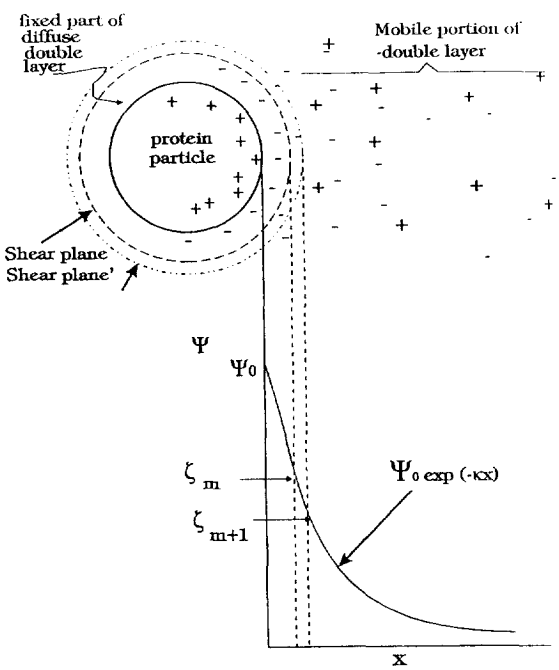

Fig. 3. A diagrammatic representation of a charged colloidal particle in an electrolyte solution, showing the relationship between the fixed and mobile parts of the diffuse double layer. Zeta potential ζ_m is the potential at the shear plane. If the shear plane was pushed outward (shear plane'), the zeta potential will decrease to ζ_{m+1}.

customary to regard the charges as a continuous distribution and to ignore individual charges. The variation of electrostatic potential with distance from a charged surface of arbitrary shape in a electrolyte solution is a classical electrostatic problem described by the Poisson–Boltzmann equation,

$$\nabla^2 \Phi = \kappa^2 \Phi \tag{1}$$

where κ is given by

$$\kappa = \left(\frac{8\pi N_0 e^2}{1\,000\,\epsilon kT}\right)^{1/2} I^{1/2} \tag{2}$$

The ionic strength, I, is sum over all molar concentrations, C_i, and charges of species in the solution:

$$I = \frac{1}{2}\sum C_i Z_i^2 \tag{3}$$

The solution of Eq. 1 describing the potential at a distance x away from a uniformly charged sphere of radius a in an electrolyte solution has the form

$$\Psi = \Psi_0 \exp(-\kappa x) \tag{4}$$

where $a >> r$, Ψ is the potential at a distance x away from the surface of the particle, Z is the charge of the particle, e is the charge of an electron, ϵ is the permittivity of the electrolyte and Ψ_0 is the potential at the Stern layer. The equation indicates that the potential drops as an exponential function of distance x from the surface of the particle. The parameter κ^{-1} has the dimension of length and is sometimes called the double layer thickness. The κ parameter regulates how fast the potential of an ion falls off in solution. And κ^{-1} is the distance within the double layer through which the potential drops 37% (1/e). It is evident from Eq. 3 that the higher the ionic strength, the more effectively the potential of an ion is screened. In a 0.1 M solution of phosphoric acid, κ^{-1} has a value of approximately 3 Å.

The mobility of a spherical molecule with radius a has been shown to be [20],

$$\mu = 2\frac{\epsilon\zeta f_1(\kappa a)}{3\eta} \tag{5}$$

where f_1 is the Henry function, which monotonically increases from 1.0 at $\kappa a = 0$ to 1.5 at $\kappa a = \infty$, in which case the equation reduces to the Helmholtz–Smoluchoski equation (Eq. 6) for the electrolysis of large smooth particles [20].

$$\mu = \frac{\epsilon \xi}{\eta} \quad (6)$$

2. Experimental

2.1. Instrumentation

All capillary electrophoresis experiments were performed on the BioFocus-3000 capillary electrophoresis system from Bio-Rad Laboratories (Hercules, CA, USA). All the capillaries used were precoated capillaries furnished in the BioFocus cartridge assembly kit (50 μm I.D. × 350 μm O.D. × 50 cm) from Bio-Rad Laboratories. The capillaries were cut to desired lengths by the user (29 cm and 50 cm, respectively). The cartridge temperature was set at 20°C. Typically, injections were made electrophoretically at 6 to 12 kV for 4 to 8 s and running voltage was 5 to 12 kV. Detection was performed by UV absorbance at 200 nm. All rhBMP-2 samples were either buffer exchanged into or diluted with 10 m*M* phosphoric acid prior to CZE analysis. The running buffer was 100 m*M* phosphate buffer, pH 2.5.

Oligomannose analysis was done on a Dionex (Sunnyvale, CA, USA) high-pH anion-exchange chromatography with pulsed amperometric detection (HPAE–PAD) system consisting of a Bio LC gradient pump, a PAD2 detector and a PA-100 (250 × 4 mm I.D.) column. Eluent A was 100 m*M* sodium hydroxide and eluent B was 100 m*M* sodium acetate in 100 m*M* sodium hydroxide. The gradient was 0% B to 100% B in 40 min. The flow-rate was 1.0 ml/min and detection was by PAD with a gold working electrode and triple-pulse amperometry.

Peptide mapping and fractionation were performed on a Hewlett-Packard (Palo Alto, CA, USA) 1090 HPLC with a Vydac (Sigma Chromatography, St. Louis, MO, USA) C_{18} or C_4 column (25 × 0.46 cm I.D.). The flow-rate was 1.0 ml/min. Solvent A was 4 m*M* heptafluorobutyric acid (HFBA), 6 m*M* trifluoroacetic acid (TFA) in water and solvent B is the same in 95% acetonitrile. The gradient was 11% B to 100% B in 75 min. Detection was at 200 nm.

Fast atom bombardment mass spectrometry was done on the HX110HF/HX110HF tandem mass spectrometer by JEOL (Peabody, MA, USA). Matrix-assisted laser desorption ionization-time of flight (MALDI-TOF) mass spectrometry was done on a Bruker (Billerica, MA, USA) REFLEX mass spectrometer equipped with a reflector.

2.2. Reagents and materials

rhBMP-2 was provided by the Genetics Institute (Andover, MA, USA). Endoproteinase Asp-N (Asp-N) was purchased from Boehringer Mannheim (Indianapolis, IN, USA). Endoglycosidase-H (Endo-H) was obtained from Genzyme (Cambridge, MA, USA). Aspergillus saitoi α(1–2)-mannosidase [α(1–2)-mannosidase] was purchased from Oxford GlycoSystems (Rosedale, NY, USA). Trifluoroacetic acid (TFA) and heptafluorobuteric acid (HFBA) and dithiothreitol (DTT) were purchased from Pierce (Rockford, IL, USA). Iodoacetic acid, sodium salt obtained from Aldrich (Milwaukee, WI, USA). Trizma Base, disodium EDTA, calcium chloride, guanidine HCl and glycerol from Sigma (St. Louis, MO, USA). HPLC grade acetonitrile was obtained from Burdick and Jackson (Muskegon, MI, USA).

2.3. Sample preparation

Endo-H digestion

rhBMP-2 and glycopeptide D5 samples were buffer exchanged into a pH 5.5, 10 m*M* sodium phosphate solution for endoglycosidase-H (Endo-H) digestion. A sample of rhBMP-2 (2.5 mg/ml) or D5 peptide was incubated with 40 mU/ml of Endo-H (specific activity = 40 U/mg) for 16 h at 37°C. The pH of the digested samples was adjusted to 2.5 using 0.1 *M* HCl before CZE analysis.

α(1–2)Mannosidase digestion

rhBMP-2 was digested to rhBMP-$2_2$$(GlcNAc)_4$-(Man5,Man5) with α(1–2)mannosidase at an enzyme/protein ratio of 50 mU/1 mg in 1 ml of sodium acetate, pH 5, at 37°C for 48 h.

Reduction and carboxymethylation of rhBMP-2

A 10-μl aliquot of 0.1 *M* dithiothreitol was added to 250 μg rhBMP-2 in 480 μl 0.5 *M* Tris buffer, 6 *M* guanidine, 5 m*M* EDTA, pH 8.5. The mixture was spun for 5 min on a bench centrifuge, layered with argon and was incubated at 37°C for 1.5 h. After the addition of 10 μl 250 m*M* iodoacetic acid, the reaction mixture incubated under argon for 1 h in darkness. The sample was immediately desalted on RP-HPLC (C_4 column) and freeze dried.

Glycan mapping

Oligomannoses were released from rhBMP-2 by Endo-H digestion. The deglycosylated protein was removed by centrifugation in a Amicon (Beverly, MA, USA) microcon-3 microconcentrator. Desalting was achieved through chromatography on a Bio-Gel P-2 column from Bio-Rad (Hercules, CA, USA) Oligomannoses were fractionated on a Dionex (Sunnyvale, CA, USA) Carbopac PA-100 column with pulsed amperometric detection. A gradient of sodium acetate from 0 to 100 m*M* over 40 min was used [21–22].

3. Results and discussion

3.1. Mobility calculations

A typical electropherogram of rhBMP-2 is shown in Fig. 4. The electropherogram shows nine peaks. The migration times of the nine peaks and their respective mobilities are summarized in Table 1. The average mobility (μ_{ave}) is 1.32×10^{-4} cm^2 V^{-1} s^{-1} and the difference in mobility between adjacent peaks ($\Delta\mu$) is 0.100×10^{-4} cm^2 V^{-1} s^{-1}. The efficiency *N* of the separation is approximately 350 000 theoretical plates per 50 cm and the resolution (R_s) is estimated to be 1.12.

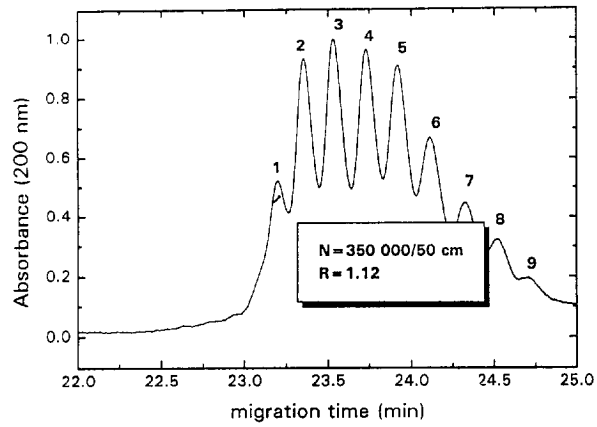

Fig. 4. CZE of rhBMP-2 in a 50 cm × 50 μm I.D. Bio-Rad, coated capillary. Sample was electroinjected for 4–8 s at 6–12 kV in 0.1 *M* phosphoric buffer (pH 2.5). Detection is by absorbance at 200 nm. Capillary cartridge temperature was controlled at 20°C.

3.2. Peak identifications

Since the polypeptide portion of rhBMP-2 is homogeneous (data not shown), its microheterogeneity is believed to come from the carbohydrate portion of the molecule. As Asn[56]SerThr is the predicted glycosylation site, we began our investigation with the glycopeptide Asp[53]-Leu[92] (D5). The D5 glycopeptide was purified from the endoproteinase Asp-N digest of reduced and alkylated rhBMP-2 using RP-HPLC. Fig. 5 compares the D5 peptide before and after Endo-H digestion. The electropherograms showed that

Table 1
Migration times and mobilities of rhBMP-2 glycoforms

Peak No.	Migration time (min)	Mobility (10^{-4} cm^2 V^{-1} s^{-1})
1	23.20	1.36
2	23.35	1.35
3	23.53	1.34
4	23.73	1.33
5	23.92	1.32
6	24.11	1.31
7	24.32	1.30
8	24.52	1.29
9	24.70	1.28

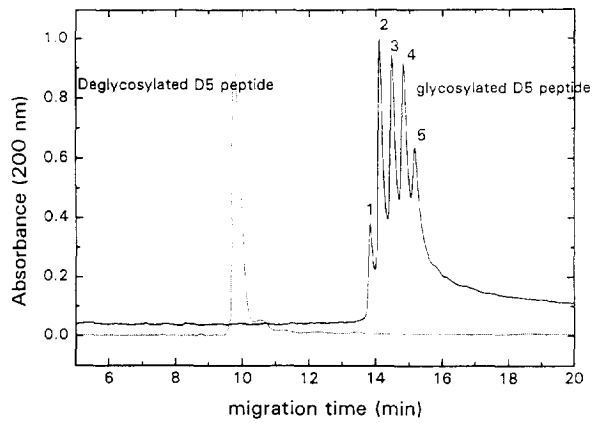

Fig. 5. Overlay of the CZE profiles of intact and deglycosylated D5 glycopeptide of rhBMP-2. A Bio-Rad, coated capillary was used. Sample was injected by electromigration for 4–8 s at 6–12 kV in 0.1 *M* phosphoric buffer (pH 2.5). Detection is by absorbance at 200 nm. Capillary cartridge temperature was controlled at 20°C.

D5 glycopeptide had five peaks before and one peak after Endo-H digestion. The collapse of the peaks by Endo-H digestion suggested that the microheterogeneity is due to a high-mannose-type carbohydrate. This postulate was confirmed by our FAB-mass spectrometric data. In order to enhance the sensitivity and accuracy of the mass spectrometric analysis, the D5 glycopeptide was further digested with endoproteinase Lys-C resulting a smaller glycopeptide Asp^{53}-K^{73}, which was recovered by RP-HPLC. Fig. 6 is the FAB-mass spectrum of the glycopeptide Asp^{53}-K^{73} [23]. The FAB-mass spectrum shows five distinct peaks. The masses correspond to the mass of the peptide (Asp^{53}-Lys^{73}) added to the masses of two N-acetylglucosamine (GlcNAc) residues and 5, 6, 7, 8 or 9 mannose residues [Asp^{53}-K^{73}-$(GlcNAc)_2Man_X$, where $X = 5$, 6, 7, 8 or 9]. That is, our MS data confirmed that the putative

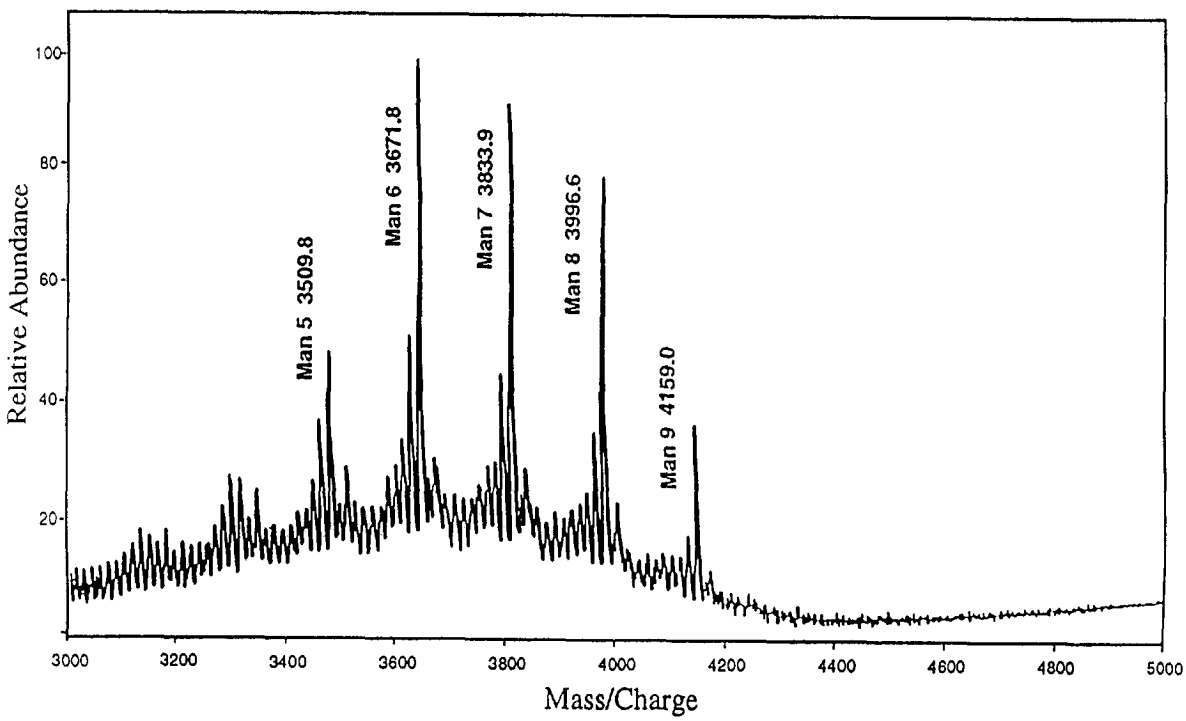

Fig. 6. Fast atom bombardment mass spectrum (FAB-MS) of the D5 glycopeptide of rhBMP-2 showing five glycoforms ($D5\text{-}(GlcNAc)_2Man_X$), where X varies from 5 to 9.

glycosylation site Asn[56] is indeed occupied by a high-mannose-type structure. The D5 electropherogram bears a striking resemblance with its FAB-mass spectrum, suggesting peak 1 to be D5-$(GlcNAc)_2Man_5$, peak 2 to be D5-$(GlcNAc)_2Man_6$, so forth. The migration pattern indicates that the D5 glycopeptide mobility decreases as mannose residues are added. The carbohydrate heterogeneity of rhBMP-2 can be further confirmed by using matrix-assisted laser desorption ionization-time of flight mass spectrometry (MALDI-TOF MS). Table 2 summarizes the mass spectrum of a reduced and alkylated rhBMP-2 sample [23]. The spectrum displayed five peaks. Strikingly, each peak in the mass spectrum corresponds to an individual glycosylation variant of the monomeric subunit. The 160 u difference between peaks is in excellent agreement with the mass of a single mannose residue ($M_r = 162$). The observed masses for all the peaks are within 0.15% of the theoretical values. This confirmed that the rhBMP-2 monomer exists in five different glycoforms rhBMP-2-$(GlcNAc)_2Man_X$, where $X = 5, 6, 7, 8$ or 9.

We now turn to intact rhBMP-2. Fig. 7 compares intact rhBMP-2 before and after Endo-H digestion. The collapse of the nine rhBMP-2 peaks into one major peak (and two minor peaks) after Endo-H digestion again confirmed that its microheterogeneity is due to the high-mannose-type carbohydrate.

Since intact rhBMP-2 is a disulfide-linked homodimer of two identical monomers, simple combinatorial calculations, $[n + c(n,r)$, where $n = 5$ and $r = 2]$ reveals that there are 15 glycoforms. The fifteen glycoforms can be represented by

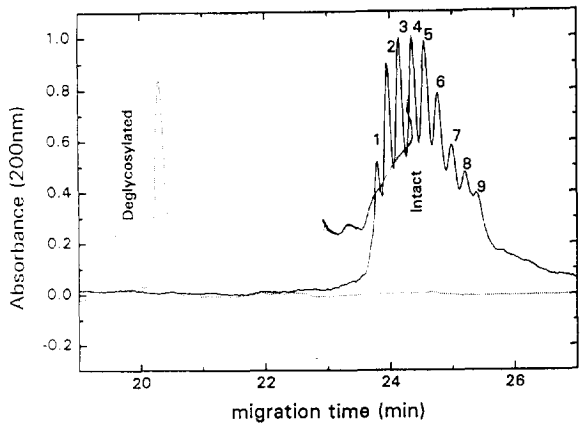

Fig. 7. Overlay of the CZE profiles of intact and deglycosylated rhBMP-2. A Bio-Rad, coated capillary was used. Sample was injected by electromigration for 4–8 s at 6–12 kV in 0.1 *M* phosphoric buffer (pH 2.5). Detection is by absorbance at 200 nm. Capillary cartridge temperature was controlled at 20°C.

the glycoform formula rhBMP-$(2)_2$-$(GlcNAc)_4$-(Man_X,Man_Y), where X and Y can vary from 5 to 9, respectively, and $X \leq Y$.

However, only nine peaks have been separated. A simple hypothesis can be proposed. If the hypothesis is confirmed, it will also shed light on the mechanism of separation. The hypothesis is: Even though there are fifteen rhBMP-2 glycoforms, there are only nine groups with distinct masses. Namely, the groups rhBMP-2_2-$(GlcNAc)_4(Man_Z)$ where Z varies from 10 to 18. Accordingly, if the CZE mechanism separates with reference to the number of mannoses a given rhBMP-2 molecule possesses, then it could only resolve nine peaks. For example, the following three glycoforms: rhBMP-$(2)_2$-$(GlcNAc)_4$-(Man_5,Man_9), rhBMP-$(2)_2$-$(GlcNAc)_4(Man_6, Man_8)$, rhBMP-$(2)_2$-$(GlcNAc)_4(Man_7,Man_7)$,

Table 2
MALDI-TOF MS results of reduced and alkylated rhBMP-2

Peak No.	Glycoform	Theoretical M_r	Observed M_r
1	BMP-2 $(GlcNAc)_2Man_5$	14 529	14 520
2	BMP-2 $(GlcNAc)_2Man_6$	14 690	14 680
3	BMP-2 $(GlcNAc)_2Man_7$	14 852	14 840
4	BMP-2 $(GlcNAc)_2Man_8$	15 014	15 010
5	BMP-2 $(GlcNAc)_2Man_9$	15 176	15 160

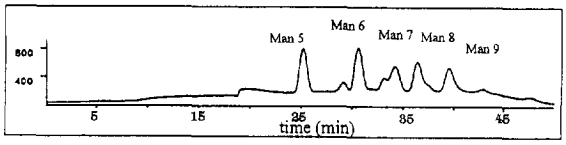

Fig. 8. High-pH anion-exchange chromatography with pulsed amperometric detection (HPAE–PAD) analysis of the N-linked oligomannose oligosaccharides released from rhBMP-2 by Endo-H digestion.

Table 3
The theoretical glycoform distribution calculated from the N-linked oligomannose analysis results

Species	Area	Fraction
M5	7.6	0.23
M6	7.5	0.23
M7	6.6	0.20
M8	6.4	0.19
M9	4.9	0.15
Species	**Isoforms**	**Fraction**
M10	55	0.05
M11	56,65	0.10
M12	57,75,66	0.14
M13	58,85,67,76	0.18
M14	59,95,68,86,77	0.20
M15	69,96,78,87	0.15
M16	79,97,88	0.10
M17	89,98	0.06
M18	99	0.02

all have 14 mannose residues each; consequently, they all have the same mobility and migrate as one peak.

3.3. Peak assignments

A theoretical glycoform distribution (the relative proportion of glycoforms) can be calculated from a rhBMP-2 glycan map. A glycan map is the high-pH anion-exchange chromatography with pulsed amperometric detection (HPAE–PAD) chromatogram of the oligosaccharides released from a glycoprotein by glycosidase digestion. A typical rhBMP-2 glycan map is shown in Fig. 8. The theoretical distribution of the rhBMP-2 glycoforms is calculated as shown in Table 3. An electropherogram of rhBMP-2 is compared to theoretical glycoform distributions I and II, as shown in Figs. 9a and 9b, respectively. In Fig. 9a, the glycoform distribution I is shown with number of mannose residues arranged in descending order. In Fig. 9b, the theoretical distribution II is shown with number of mannose residues arranged in ascending order. The similarity between the CZE profile and theoretical distribution II suggests that the peak assignments in Fig. 9b are correct. In other words, the migration time increases (or the mobility decreases) as the number of mannoses is increased.

However, an independent verification is still

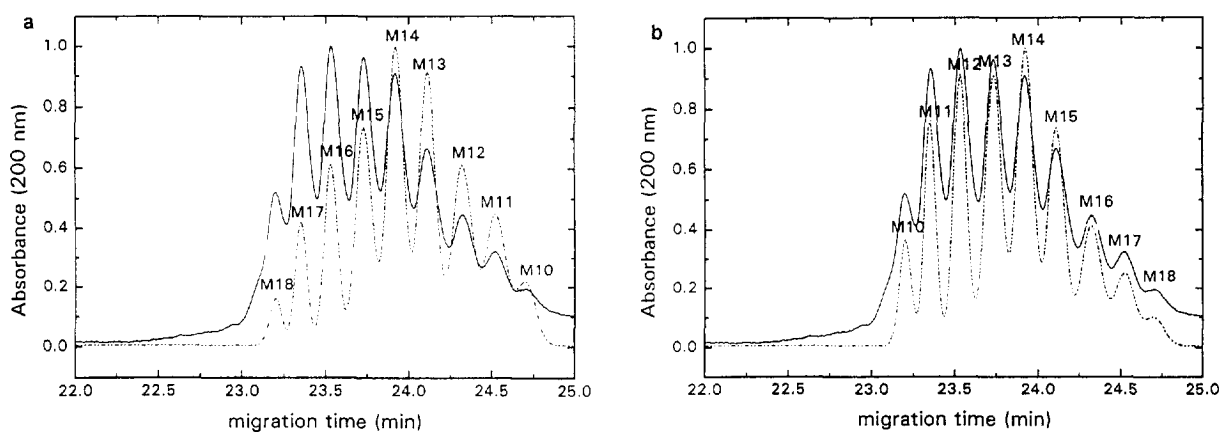

Fig. 9. (a) Comparison of the CZE profile of rhBMP-2 with the theoretical glycoform distribution I calculated from the oligosaccharides analysis results. (b) Comparison of the CZE profile of rhBMP-2 with the theoretical glycoform distribution II calculated from the oligosaccharides analysis results.

required. A direct proof can be realized if an enzyme which can convert all rhBMP-2 glycoforms to (rhBMP-2)$_2$-(GlcNAc)$_4$(Man$_5$,Man$_5$) can be found. Fortunately, such an enzyme does exist and it is α(1–2)mannosidase. As shown in Fig. 10, when rhBMP-2 is digested with α(1–2)mannosidase, the cluster of nine peaks does collapse into a single peak coincident with the (rhBMP-2)$_2$-(GlcNAc)$_4$(Man$_5$,Man$_5$), thus confirming the peak assignments.

3.4. Mobility depends on the number of mannoses

When the mobilities and migration times of the rhBMP-2 glycoforms are plotted against the numbers of mannose residues, two straight lines with $R^2 > 0.999$ result. Two observations can be made from these results. Firstly, the mobility of a given glycoform decreases when its number of mannose residues increases. Secondly, the slope $\delta\mu/\delta n|_n$ is constant and is equal to $0.1 \cdot 10^{-4}$ cm^2 V^{-1} s^{-1}.

Since rhBMP-2 is homogeneous in charge and oligomannoses are neutral, the rhBMP-2 glycoforms are not expected to be resolved by CZE as there are no charge differences. But, interestingly enough, nine peaks were indeed resolved and it is important to examine possible mechanisms of separation. In other words, how does an incremental mannose residue affect the mobility of rhBMP-2?

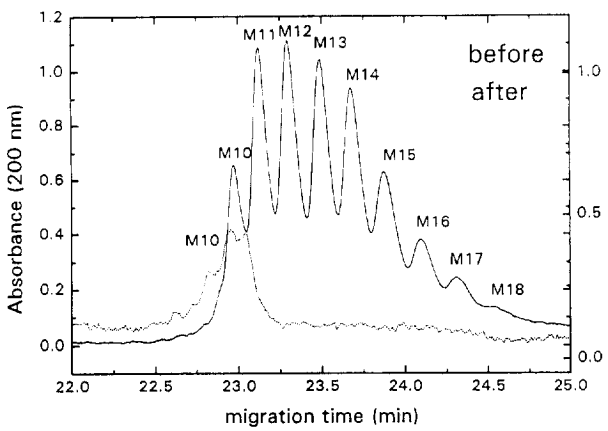

Fig. 10. Overlay of the CZE profiles of intact and α(1–2)-mannosidase digested rhBMP-2. rhBMP-2 was digested to rhBMP-2 oligomannose 10 with α(1–2)mannosidase at an enzyme–protein ratio of 50 mU/mg in 1 ml of sodium acetate, pH 5, at 37°C for 48 h.

3.5. Plausible mechanisms

Since mobility of a particle is defined as

$$\mu = \frac{q}{f} \tag{7}$$

where μ is the mobility of a particle, q is its surface charge and f its frictional coefficient. A neutral mannose molecule can reduce the mobility of rhBMP-2 by increasing its frictional coefficient or decreasing its effective charge.

Effect of mass of a mannose on rhBMP-2 mobility

rhBMP-2 belongs to the transforming growth factor β (TGF-β) family of growth factors and is believed to have a rod shape like TGF-β. If we assume rhBMP-2 to have a rod shape, then its frictional coefficient should be proportional to its molecular mass (M_r) raised to the power 0.8 [24]. After substituting $M^{0.8}$ for f, differentiating Eq. 4 and noting that charge q is constant, we obtain

$$\frac{d\mu}{\mu} = -0.8\frac{dm}{m} \tag{8}$$

This equation states that the fractional change in mobility is equal to eight tenths the fractional change in molecular mass. Given that the mass of a mannose is 162 and that the mass of rhBMP-2$_2$-(GlcNAc)$_4$Man$_{14}$ is 29 680, the fractional mass change (dm/m) is 162/29 680 or 0.54%,. Thus, the calculated fractional change in mobility ($\Delta\mu_f/\mu$) is ($-0.8 \times 0.54\%$) or -0.43%. Since the experimentally determined fractional change in mobility ($\Delta\mu_f/\mu$) is $(-0.100 \cdot 10^{-4}$ cm^2 V^{-1} s^{-1})/($1.32 \cdot 10^{-4}$ cm^2 V^{-1} s^{-1}) = -0.75%, the incremental mass change of a mannose can account for (0.43/0.75) = 57% of the observed

mobility change ($\Delta\mu$) on rhBMP-2 through its effect on the frictional coefficient f.

Effect of one charge on rhBMP-2 mobility

Fig. 11 is the electropherogram of a mixture two rhBMP-2 charge variants. The two charge variants arise because the N-terminal of rhBMP-2 is a glutamine (Gln form) which can cyclize to form a pyroglutamic acid (pyroglu form). The Gln terminus is positively charged under acidic conditions while the pyroglu terminus is not; so there is a two-charge difference between the two forms (rhBMP-2 being a dimer). The mobility differences between the corresponding pair of glycoforms should be attributable to their charge differences alone. In other words, since the charge difference between the $(\text{Gln-rhBMP-2})_2$-$(\text{GlcNAc})_4\text{Man}_{10}$ and $(\text{pyroglu-rhBMP-2})_2$-$(\text{GlcNAc})_4\text{Man}_{10}$ forms is two charges, the 'effective charge difference' between adjacent glycoforms can be estimated to be 0.51 charges. In other words, adding a mannose to rhBMP-2 has the same effect on its mobility as reducing its total charge by 0.51.

By using a simple particle model, we can already gain insight on how a mannose residue can affect the mobility of rhBMP-2 through a charge shielding effect, hydrodynamic drag (f) effect, or a combination of the two.

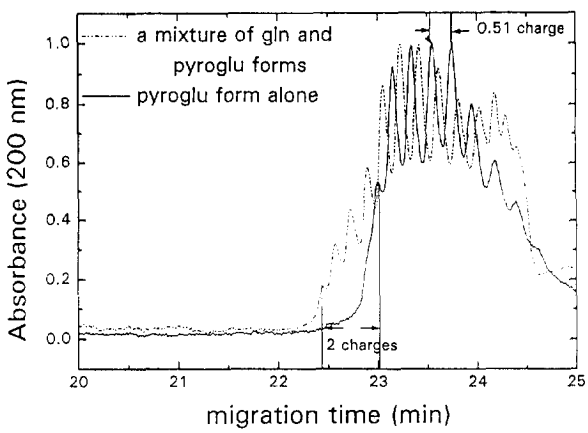

Fig. 11. Overlay of the CZE profiles of a mixture of the pyroglu and gln forms of rhBMP-2 and that of the pyroglu form of rhBMP-2.

It is difficult to ascribe a meaning to the charges on a colloid particle; it is more useful to consider the electrostatic potential on its surface. From the mobilities of the rhBMP-2 glycoforms, their respective zeta potentials can be calculated. Substituting $\eta = 0.010$ P and $\epsilon = 80.4$ for water at 20°C into Eq. 6, the zeta potential, ζ, of $(\text{rhBMP-2})_2$-$(\text{GlcNAc})_4(\text{Man}_5\text{Man}_5)$ is 38 mV and $\Delta\zeta$ is -0.29 mV per mannose residue. One interpretation is that, as shown diagrammatically in Fig. 3, the zeta potential ζ of a particle is the potential at its 'surface of shear' or 'slip plane'. The location of the 'slip plane' or 'surface of shear' is not known independently, but it seems reasonable that it is not far away from the Stern plane. It fact, it is often assumed that they coincide, and that $\psi_0 \approx \zeta$. It is likely that the slip plane is just slightly further out into the outer edge of the Stern layer. The potential ζ depends on all those things that fix the structure of the diffuse double layer, including the presence of neutral species. The addition of the mannose units to rhBMP-2 has the effect of extending the shear plane outward, reducing the zeta potential by 0.29 mV. Whether the incremental mannose residue extends the shear plane further into the double layer, thus reducing the zeta potential, or the incremental mannose residue increases the frictional coefficient of the particle and at the same time shields and reduces the 'effective charge' on the protein particle cannot be discerned. Both the charge and hydrodynamic factors seem to be involved.

It is illuminating to examine Fig. 12, which is the X-ray crystal structure of TGF-β2 [25,26] drawn on the same scale with an oligomannose 9 structure, to obtain an appreciation of their spatial arrangement. The reader can almost mentally form a bond between Asn^{56} and the N-acetylglucosamine of the oligomannose 9 structure. The most salient feature of the structure is that the oligomannose 9 structure is large relative to the protein, considering its molecular mass. One consequence of this large size is that the oligomannose may conceivably wrap around

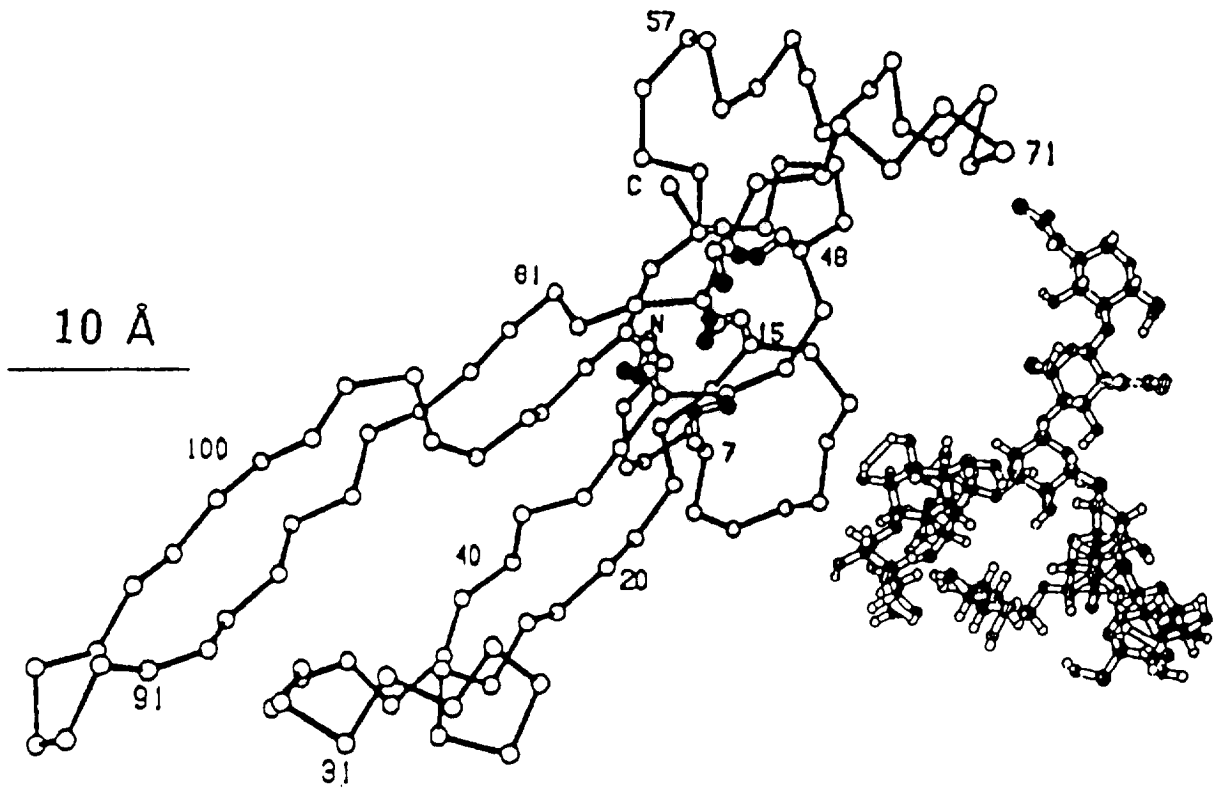

Fig. 12. X-ray crystal structures of TGF-β2 and an oligomannose 9 ($GlcNAc_2Man_9$).

the N-terminal region (where numerous positive charges are located) and as a result reduces the 'effective charge' on the protein particle.

4. Conclusion

We have shown that recombinant human bone morphogenetic protein 2 (rhBMP-2) has fifteen glycoforms. Their structures can be described by the formula $(rhBMP\text{-}2)_2\text{-}(GlcNAc)_4(Man_X, Man_Y)$, where $X \leq Y$ and X and Y can vary from 5 to 9, respectively. We have separated the fifteen glycoforms into nine peaks. The identities of the nine peaks are $(rhBMP\text{-}2)_2\text{-}(GlcNAc)_4(Man_X,Man_Y)$ where $X + Y = 10,11,\ldots,18$. In other words, we were able to separate two proteins ($M_r \approx 30\,000$) that differ by only one mannose residue. We were not able to separate the rhBMP-2 glycoforms that have the same number of mannose residues (stereoisomers). Since mannose is a neutral molecule and the protein is homogeneous, all the rhBMP-2 glycoforms have the same charge and were not expected to be separated without resorting to chemical complexation. We explored several separation mechanisms and concluded that the size of the mannose residue is the key to the separation mechanism. The mannose residue is large compared to the size of a protein. Consequently, it either provides enough drag or shields enough charges on the molecule to reduce its mobility to be resolved. Since the slope of the mobility versus number of mannose plot $(\delta\mu/\delta n|_n)$ is so constant, we believe the drag effect rather than charge shielding to be primarily responsible for the decrease in mobility. The

novelty of our separation is that no complexation is invoked and all the glycoforms carry the same charge. Based on our results, we can infer that CZE using a simple low-pH buffer can resolve not only glycoforms with uncharged (neutral) glycans but also glycoforms with charged glycans (sialylated species for example) [4]. Therefore, CZE under low-pH conditions, when the proteins are fully positively charged, is a technique uniquely suitable for complex glycoform analysis without resorting to complexation reactions.

Acknowledgements

The authors would like to thank Leah Abraham, Yangkil Kim and Bi Xu for technical assistance; Dr. John Steckert, Dr. David Williams, Dr. Michael Yet, and Dr. Brian Tripp for valuable discussions; and the Structural Biochemistry group at the Genetics Institute for the mass spectral data and the sequence diagram for rhBMP-2. The authors would specially like to thank Dr. Richard Kenley and Dr. Godfrey Amphlett for their support.

References

[1] A. Variki, Glycobiology, 3 (1993) 97.
[2] S. Dube, J.W. Fischer and J.S. Powell, J. Biol. Chem., 263 (1988) 17516.
[3] M. Takeuchi and A. Kobata, Glycobiology, 1 (1991) 337.
[4] K.W. Yim, J. Chromatogr., 559 (1991) 401.
[5] A.D. Tran, S. Park, P.J. Lisi, O.T. Huynh, R.R. Ryall and P.A. Lane, J. Chromatogr., 480 (1989) 351.
[6] F. Kilar and S. Hjerten, Electrophoresis, 10 (1989) 23.
[7] S.L. Wu, G. Teshima, J. Cacia and W.S. Hancock, J. Chromatogr., 516 (1990) 115.
[8] J.P. Landers, Anal. Biochem., 205 (1992) 115.
[9] R.P. Oda, B.J. Madden, T.C. Spelsberg and J.P. Landers, J. Chromatogr. A, 680 (1994) 85.
[10] P.M. Rudd, H.C. Joao, E. Coghill, P. Fiten, M.R. Saunders, G. Opdenakker and R.A. Dwek, Biochemistry, 33 (1994) 17.
[11] P.M. Rudd, I.G. Scagg, E. Coghill and R.A. Dwek, Glycoconjugate J., 9 (1992) 86.
[12] H.C. Joao, I.G. Scagg and R.A. Dwek, FEBS Lett., 307 (1992) 343.
[13] E.A. Wang, V. Rosen, P. Cordes, R.M. Hewick, M.J. Kriz, D.P. Luxemberg, B.C. Sibley and J.M. Wozney, Proc. Natl. Acad. Sci. USA, 85 (1988) 9484.
[14] J.M. Wozney, V. Rosen, A.J. Celeste, L.M. Mitsock, M.J.Whitters, R.W. Kriz, R.M. Hewick and E.A. Wang, Science, 242 (1988) 1528.
[15] A.J. Celeste, J.A. Iannazzi, R.C. Taylor, V. Rosen, E.A. Wang and J.M. Wozney, Proc. Natl. Acad Sci. USA, 87 (1990) 9843.
[16] J.M. Wozney, Prog. Growth Factor Res., 1 (1989) 267.
[17] E.A.Wang, V. Rosen, J.S. D'Alesandro, M. Bauduy and J.M. Wozney, Proc. Natl. Acad. Sci. USA, 87 (1990) 2220.
[18] A.W. Yasko, J.M. Lane, J.M. Wozney, V. Rosen and E.A.Wang, J. Bone Joint Surg., 74 (1992) 659.
[19] D.M. Touiumi, H.S. Kotler, D.P. Luxenberg and E.A. Wang., Arch. Otolaryngol. Neck Surg., 117 (1991) 1101.
[20] P.C. Hiemenz, Principles of Colloid and Surface Chemistry, Marcel Dekker, New York, 1991.
[21] M.R. Hardy and R.R. Townsend, Proc. Natl. Acad. Sci. USA, 85 (1988) 3289.
[22] Y.C. Lee, Anal. Biochem., 189 (1990) 151.
[23] M.D. Bond, M.A. Jankowski, S.A Martin and H.A. Scoble, Sixth International Symposium of the Protein Society, San Diego, CA, 1992, abstract.
[24] C.R. Cantor and P.R. Schimmel, Biophysical Chemistry, Freeman, New York, 1980.
[25] S. Daopin, K.A. Piez, Y. Ogawa and D. Davies, Science, 257 (1992) 369.
[26] S. Daopin, M. Li and D.R. Davies, Proteins: Structure, Function and Genetics, 17 (1993) 176.